DOI: 10.1002/ejoc.200601128

# Secondary Metabolites Isolated from an Endophytic *Phoma* sp. – Absolute Configuration of Tetrahydropyrenophorol Using the Solid-State TDDFT CD Methodology[‡]

**Karsten Krohn,*[a] Umar Farooq,[a] Ulrich Flörke,[a] Barbara Schulz,[b] Siegfried Draeger,[b] Gennaro Pescitelli,[c] Piero Salvadori,[c] Sándor Antus,[d,e] and Tibor Kurtán[d]**

**Keywords:** Fungal metabolites / Pyrenophorol / Tetrahydropyrenophorol / Pyrenophorolic acid / Antifungal activity / Algicidal activity / Absolute configuration / Solid-state TDDFT CD methodology / CD sector rules

The known macrolide pyrenophorol (synonym helmidiol) (**1**), the new 2,3,10,11-tetrahydropyrenophorol (**3**), and (4*S*,7*R*)-4,7-dihydroxyoctanoic acid (**4**), the monomeric acid of the sixteen-membered cyclic diolide **1**, were isolated from an endophytic *Phoma* sp. The relative configuration of tetrahydropyrenophorol (**3**) was confirmed by X-ray single crystal analysis and its absolute configuration determined by the solid-state TDDFT CD methodology. Compounds **1** and **4** show antifungal activity and the acid **4** is also an algicide.



## Introduction

As part of our continuing investigations of new bioactive metabolites from fungi, we analyzed the ethyl acetate culture extract of an endophytic *Phoma* sp., isolated from the plant *Fagonia cretica*, from Gomera (Spain). The fungus was cultivated on 12 L of biomalt solid agar media for 25 d at room temperature. The crude extract showed good herbicidal and algicidal and moderate fungicidal activities. Silica gel column chromatography of the crude culture extract resulted in the isolation of three metabolites, **1**, **3**, and **4** (Figure 1). The structure of the new tetrahydropyrenophorol (**3**) was elucidated by spectroscopic methods and X-ray structure analysis. Its absolute configuration was assigned by comparison of the solid-state CD spectrum with that computed by means of the TDDFT method, using the geometric crystal structure data as input for the calculations.

## Results and Discussion

An optically active ($[\alpha]_D$ = –13.3) metabolite of medium polarity was isolated as colorless crystals with m.p. 130–132 °C. The molecular formula $C_{16}H_{24}O_6$ resulted from EIMS ($M^+/2$ = 156, $C_8H_{12}O_3$) in conjunction with the NMR spectra. In the IR spectrum, the peaks at 3325 and 1716 $cm^{-1}$ indicated the presence of hydroxy groups and a carbonyl group, respectively. Analysis of the $^1H$-, $^{13}C$-, and 2D ($^1H$-$^1H$-COSY and $^1H$-$^{13}C$-HETCOR) NMR and mass spectroscopic data and comparison with literature values revealed the identity with pyrenophorol (**1**) (Figure 1). The similar specific optical rotation in chloroform of our product with the reported value ($[\alpha]_D$ = –14.9)[2] indicated the same absolute configuration for the two samples. Interestingly, the optical rotation of pyrenophorol is strongly dependent on the solvent used and even shows opposite optical rotation in methanol and chloroform, possibly due to its solvent-dependent conformational flexibility.[3] Pyrenophorol (**1**) was isolated first from the fungus *Byssochlamys nivea*,[4] and shortly later from *Stemphylium radicinum*.[5] It is closely related to the corresponding diketone pyrenophorin (**2**)[6–8] which was shown to have good herbicidal activity.[9] Later the diolide **1** was also isolated from the imperfect fungus *Alternaria alternata* and named helmidiol.[2] The identity of pyrenophorol with helmidiol, exhibiting pronounced anthelmintic properties,[10] was shown by Australian workers, who also confirmed the relative configuration of **1** by X-ray structure analysis.[6] A sample of helmidiol kindly provided by A. Zeeck (University of Göttingen) was identical to our compound **1**. The absolute (4*S*,7*R*,4′*S*,7′*R*)-configuration of pyrenophorol (**1**) as well as the (7*R*,7′*R*)-configuration of pyrenophorin (**2**) were es-

[‡] Biologically Active Secondary Metabolites from Fungi, 28. Part 27: Ref.[1]

[a] Department of Chemistry, University of Paderborn, Warburger Straβe 100, 33098 Paderborn, Germany
Fax: +49-5251-60-3245
E-mail: k.krohn@uni-paderborn.de
[b] Institut für Mikrobiologie, Technische Universität Braunschweig, Spielmannstraße 7, 31806 Braunschweig, Germany
[c] Università di Pisa, Dipartimento di Chimica e Chimica Industriale, via Risorgimento 35, 56126 Pisa, Italy
[d] Department of Organic Chemistry, University of Debrecen, P. O. Box 20, 4010 Debrecen, Hungary
[e] Research Group for Carbohydrates of the Hungarian Academy of Sciences, P. O. Box 55, 4010 Debrecen, Hungary

Supporting information for this article is available on the WWW under http://www.eurjoc.org or from the author.

  

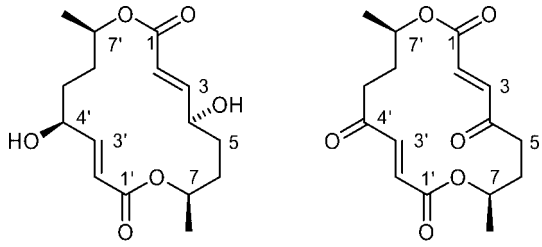


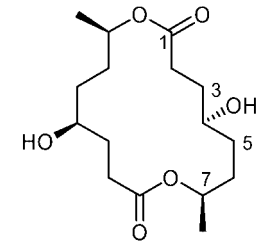


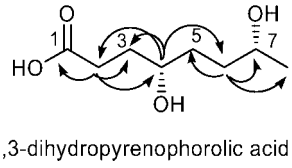


Figure 1. Molecular structures of pyrenophorin (**2**) and of the secondary metabolites **1**, **3**, and **4** isolated from *Phoma* sp., and HMBC correlation of **4**.

tablished by several enantioselective syntheses[11–14] and also by the synthesis of *ent*-**1**.[15]

In addition to the known pyrenophorol (**1**), we also isolated a new member of the family, the tetrahydro derivative **3** as the least polar component from the fermentation. The product crystallized from dichloromethane/petroleum ether with m.p. 124–127 °C and had much higher levorotatory specific optical rotation ($[\alpha]_D$ = –68) than **1**. The EIMS [M + $H^+$/2] with *m*/*z* = 159 for $C_8H_{14}O_3$ showed half of the symmetrical dimeric molecule as did the NMR spectra with 8 signals in the $^{13}C$ NMR and 14 proton signals in the $^1H$ NMR spectra. The IR spectrum showed absorption for the hydroxy group at 3418 $cm^{-1}$ and carbonyl carbon at 1732 $cm^{-1}$. The presence of a signal for a secondary methyl group, $\delta$ = 1.23 ppm (d, 3 H, *J* = 6.2 Hz, H-8), attached to a methine group, $\delta$ = 5.03 ppm (m, 1 H, H-7), bearing the oxygen atom of the lactone bridge, was seen in the $^1H$ NMR spectrum. The geminal proton of a secondary hydroxy group gave rise to a signal at $\delta$ = 3.56 ppm (m, 1 H, H-4), and four methylene groups to signals centered at $\delta$ = 2.45 (m, 2 H, H-2), 1.86 (m, 1 H, H-6), 1.79 (m, 1 H, H-6), 1.72 (m, 2 H, H-3), 1.52 (m, 1 H, H-5), and 1.37 ppm (m, 1 H, H-5). The positions of the substituents in the C-1 to C-8 carbon chains resulted unambiguously from the cross peaks in the $^1H$-$^1H$ COSY spectrum. The $^{13}C$ NMR spectrum disclosed the presence of one secondary methyl signal appearing at $\delta$ = 20.0 ppm, four methylene signals centered at $\delta$ = 33.1 (C-3), 31.1 (C-6), 30.8 (C-5) and 30.7 ppm (C-2). The methine signals resonated at $\delta$ = 69.6 (C-7) and 68.0 (C-4), while the signal for the carbonyl carbon appeared at $\delta$ = 173.4 ppm (C-1). The HMBC experiments showed $^1H$-$^{13}C$ correlations of the methine proton at $\delta$ = 5.03 ppm (H-7) with C-1 ($\delta$ = 173.4 ppm), C-6 ($\delta$ = 31.1 ppm), and C-8 ($\delta$ = 20.0 ppm). The correlations between H-4 ($\delta$ = 3.56 ppm) and C-6 ($\delta$ = 31.1 ppm), C-5 ($\delta$ = 30.8 ppm), and C-3 ($\delta$ = 33.1 ppm) were also observed. Similarly, the methylene signal for H-2 ($\delta$ = 2.45 ppm) showed connectivity with C-1 ($\delta$ = 173.4 ppm), C-4 ($\delta$ = 68.0 ppm) and C-3 ($\delta$ = 33.3 ppm). Since the MS and $^1H$- and $^{13}C$-NMR data presented only signals for half of the symmetric diolide molecule **3**, its structure, including the relative stereochemistry, was unambiguously confirmed by X-ray analysis (Figure 2). The quality of anisotropic displacement parameters is very good. Except for O1 and, to a lesser extend, O4, all other non-hydrogen atoms show largely isotropic behaviour.

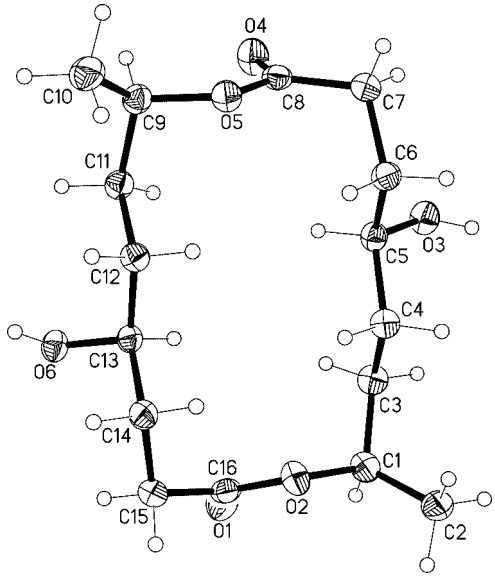


Figure 2. The molecule of tetrahydropyrenophorol (**3**) in the crystal.

## Absolute Configuration of Tetrahydropyrenophorol (3): Solid-State CD/TDDFT Approach

Although biosynthetic considerations suggest the same absolute configuration for **1** and **3**, an independent proof of the absolute configuration of compound **3** can be provided by our new solid-state TDDFT CD methodology.[16–18] Assignment of the absolute configuration of compound **3** by means of quantum-mechanical CD calculations[19] and comparison with the experimental CD would be a formidable task if the solution structure had to be considered. For the 16-membered saturated ring there is ample scope for a great number of conformations to be populated at room temperature. Prediction of all possible conformations necessarily limits the range of practicable computational methods to molecular mechanics or semi-empirical calculations. Consequently, the estimation of relative free

  

energies would be severely flawed. Moreover, geometry optimization of each conformer with the DFT method, and calculation of the CD spectrum[20,21] for each optimized structure with the TDDFT method,[22,23] would both be excessively costly. Conformational studies on **3** with MMFF and AM1 methods resulted in several minima with low energy. For example, after using AM1, 10 minima were found within 1 kcal/mol, 32 within 2 kcal/mol, about 60 within 3 kcal/mol. Among these, the structure corresponding to the solid-state was found as the 13th most stable (+1.2 kcal/mol AM1 energy with respect to the absolute minimum), although the 4th most stable (+0.17 kcal/mol) was also very similar. These results are nicely corroborated (vide infra) by the noteworthy experimental observation (Figure 3) that the CD spectra measured for **3** in solution (acetonitrile or methanol) and in the solid state (as KCl disc) differ in sign and, slightly, in the position of the prominent band due to carbonyl *n*-π* transitions. Clearly, the conformational ensemble populated at room temperature in solution is *not* well represented by the structure isolated in the solid state, otherwise the observed discrepancy could hardly be rationalized. In fact, in the current case, CD effects intrinsic to the solid state, arising for example from intermolecular couplings, will be negligible due to the nature of the diagnostic transitions involved, i.e., *n*-π*, which are electric-dipole forbidden and very local in character. All the necessary precautions were taken to exclude the presence of artefacts allied to the solid sample. The effect of the rotation-dependent macroscopic anisotropy of the KCl disc was checked by sample rotation. CD spectra were recorded with 0°, 90°and 180° rotations about the propagation of light (Z axis) which resulted in only slightly different spectra of high S/N ratio.[24] Due to the electric-dipole forbidden n-π* transition, the $\Delta\varepsilon/\varepsilon$ ratio is relatively high which allowed a higher concentration of the sample in the KCl disc and hence a larger CD signal without exceeding absorbance or HT limit.

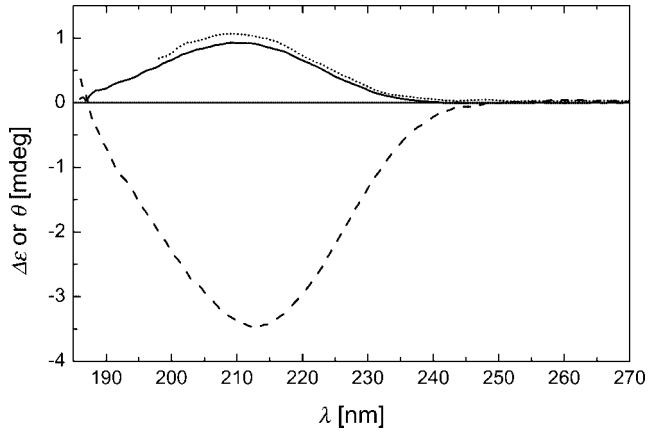


Figure 3. CD spectra of tetrahydropyrenophorol (**3**) measured in acetonitrile (solid line), methanol (dotted line) and as KCl disc (broken line).

Compound **3** represents therefore an ideal example for which our solid-state CD/TDDFT approach is most valuable.[17,18] In this case only a single structure, available from X-ray analysis, needs to be considered for the CD calculation, so that the entire conformational study step may be skipped.

Figure 4 reports the CD spectra computed with the TDDFT method at the B3LYP/TZVP level for the solid-state structure of **3** with (4*S*,7*R*,4′*S*,7′*R*) absolute configuration. Above 185 nm, the calculated spectrum consists of a single negative band arising from the summation of the two *n*-π* transitions at 209 and 215 nm, corresponding to the excitations from the two highest occupied Kohn–Sham orbitals to the two lowest virtual orbitals. The two transitions are almost, but not exactly, degenerate because the solid-state structure is only close to $C_2$ symmetry (the root-mean-square deviation from the closest symmetric structure is 0.040 Å for all atoms and 0.028 Å for heavy atoms only). The two transitions have computed oscillator and rotational strengths $f \approx 0.002$ and $R$ –7.1/–6.9 × $10^{-40}$ cgs, respectively. They are well isolated from the following ones at high energy (the next one is calculated at 181 nm), and have energies (around 5.83 eV) well below the TDDFT-estimated ionization potential (7.42 eV).[25] These considerations and the very good match between calculated and recorded CD spectra in the solid state (experimental $\lambda_{max}$ = 212 nm) clearly suggest the (4*S*,7*R*,4′*S*,7′*R*) configuration for compound **3**. In addition, this assignment is in agreement with the absolute configuration of compound **1**, isolated from the same source.

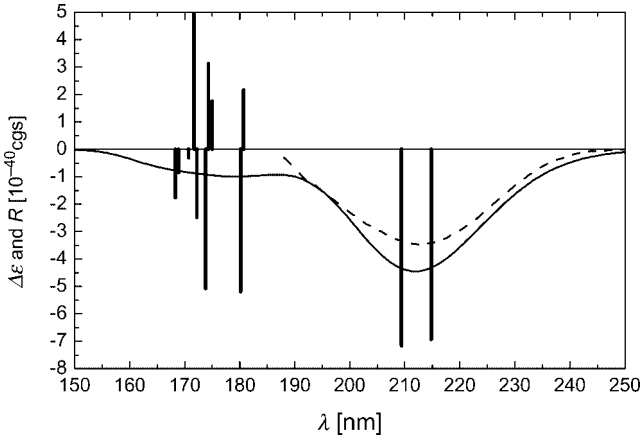


Figure 4. TDDFT-calculated CD spectrum (B3LYP/TZVP method) for (4*S*,7*R*,4′*S*,7′*R*)- tetrahydropyrenophorol (**3**) using the solid-state geometry; vertical bars represent rotational strengths *R*. Broken line: experimental solid-state spectrum shown for comparison.

Although the *n*-π* transitions seem to be very well predicted with the B3LYP/TZVP method, it was worth testing the performance of other exchange-correlation functionals, as well as the effect of larger basis sets.[26] Using the TZVP basis set, the PBE0 functional led to results comparable to B3LYP ($\lambda$ = 207/212 nm, $R$ = –7.2/–6.8, in $10^{-40}$ cgs units), while the BH&HLYP functional, with increased HF exchange character, was slightly less satisfactory ($\lambda$ = 198/203 nm, $R$ = –7.0/–6.3). TZVP, a triple-ζ split-valence basis set with no diffuse functions,[26] is our first choice for

  

TDDFT calculations in the view of a very favourable accuracy/cost trade-off observed in most situations.[17,18,27] However, in the current case, we noticed some inconsistency between rotational strengths computed with dipole-length (DL) and dipole-velocity (DV) gauge formulations:[20,21,28] DL and DV values for the two diagnostic transitions differed by 15–20% (depending on the functional employed). Since this is indication of basis set incompleteness,[20,21,28] we ran additional calculations using B3LYP with two larger basis sets: 1) aug-cc-pVDZ, a correlation-consistent double-ζ basis set augmented with diffuse functions; 2) aug-TZVP, i.e., TZVP augmented with the same set of diffuse functions as of aug-cc-pVDZ.[26] They led to an almost complete coincidence between DL and DV values (discrepancies within 2–3%), but not to substantial differences in the computed CD spectrum (aug-cc-pVDZ: $\lambda$ = 212/217 nm, $R$ = –10.2/–9.3; aug-TZVP: $\lambda$ = 211/217 nm, $R$ = –10.0/–9.0) with respect to B3LYP/TZVP.

Incidentally, it was worth checking the sign of the experimental (and TDDFT-computed) $n$-π* CD band for compound **3** against the available semi-empirical sector rules for $n$-π* transitions of chiral esters and lactones. Our intention is to stress that the current solid-state TDDFT/CD methodology may be of great help for a critical evaluation of established semi-empirical spectra-structure relationships.[29,30] In fact, the two fundamental prerequisites of such approaches, that is, 1) a fixed and known molecular conformation, and 2) a well-characterized and isolated electronic transition, may be safely verified in the context of the solid-state TDDFT/CD method. In the current case, the CD band observed at 210 nm is due to almost pure $n$-π* transitions; the negative sign recorded for (4*S*,7*R*,4′*S*,7′*R*)-**3** in the rigid solid-state geometry is in agreement with that predicted by Snatzke's sector ("comet") rule for esters.[31,32] Since sector rules usually take into special consideration the perturbing groups closest to the chromophore (belonging here to the so-called third chiral sphere),[30] we analyzed the "chirogenic" fragment **5** (Figure 5) obtained from **3** by cutting the carbon chains at each second carbon atom from one ester group, and retaining the same conformation as in the solid-state structure of **3**. With B3LYP/aug-cc-pVDZ, the $n$-π* transition was computed for **5** at 219 nm with $R$ $-11.2 \times 10^{-40}$ cgs, in close agreement with the results obtained for the single transitions of the entire molecule **3**. This result proves that the three methyl groups in **5** do in fact represent the main perturbers responsible for the observed optical activity of **3**. Upon systematic variations of the main dihedral angles in **5**, we could modify the reported rule[31,32] as indicated in Figure 5, the main difference lying in the shape of the upper curved nodal surface. We believe that such analyses may help rejuvenate some sector rules that have been very popular in the past and still represent, in our opinion, useful tools for a quick interpretation of CD spectra.

In fact, the modified sector rule facilitated the investigation of the origin of the marked difference observed between solution and solid-state CD spectra (Figure 3). We considered the two chirogenic moieties, analog to **5**, extracted from each of the lowest 32 structures computed with AM1 for **3**. They feature a large variation in the relevant dihedral angles and therefore in the position of the methyl groups. Application of the modified "comet" rule led to an estimate of an overall positive CD in the $n$-π* region for 12 over 32 structures, a negative CD for 14, and a negligible CD for 6. For the first ten structures, these predictions were confirmed through TDB3LYP/3-21G(d) computations (see electronic supporting information). Thus, the large molecular flexibility in solution must be deemed responsible for a measured average CD spectrum with sign opposite to the solid-state one, this latter allied to a single conformation.

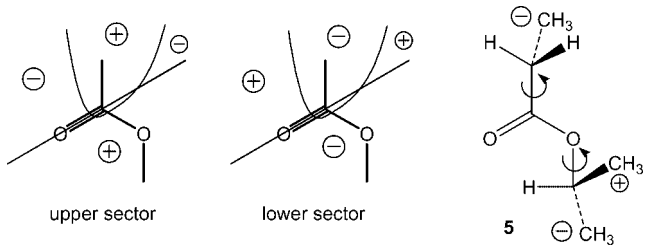


Figure 5. Snatzke's sector "comet" rule for esters[31,32] modified according to TDDFT calculations (B3LYP/TZVP level) on the chirogenic fragment **5** with various orientations of the methyl groups, obtained by systematic variations of the two indicated dihedrals. The signs show contributions to $n$-π* transition for groups lying in each sector.

The most polar compound, a C-8 chain carboxylic acid, was isolated as a colorless oil with similar specific optical rotation ($[\alpha]_D$ = –71.7) as found for diolide **3**. Its molecular formula was established as $C_8H_{16}O_4$ by a $[M + H]^+$ peak at $m/z$ = 177 in the mass spectrum (EIMS), supported by the NMR spectra with 8 signals in the $^{13}C$ NMR and 14 proton signals in the $^1H$ NMR spectra. The $^1H$ NMR showed a signal of a secondary methyl group at $\delta$ = 1.22 (d, 3 H, $J$ = 7 Hz, H-8), attached to a methine group (signal centered at $\delta$ = 3.86 ppm, m, 1 H, H-7) bearing a hydroxy group. The signal of a geminal proton of a secondary hydroxy group appeared at $\delta$ = 4.55 (m, 1 H, H-4), the four methylene groups gave rise to peaks at 2.54 (m, 2 H, H-2), 2.34 (m, 1 H, H-3), 1.90 (m, 1 H, H-3), 1.87 (m, 1 H, H-5), 1.71 (m, 1 H, H-5), and 1.55–1.64 ppm (m, 2 H, H-6). Based on the $^1H$-$^1H$ COSY spectrum and HMBC correlations (see Figure 1), the connectivity of the C-1 to C-8 chain was established in agreement with the planar structure of 4,7-dihydroxyoctanoic acid (pyrenophorolic acid) (**4**). Evidently, acid **4** is the monomer of the dimeric diolide **3** and it is reasonable to assume the same relative and absolute configuration for **4** as established for **3**.

Symmetric diolide structures are relatively rarely observed as natural products. Recently, we found a $C_3$-symmetric 24-membered tris-lactone, dasypogalactone, from the Indonesian lichen *Usnea dasypoga* Rohl[33] whose relative stereochemistry could be established by X-ray structure analysis.[34] 16-Membered dilactones of the pyrenophorol type are found in pyrenophorin (**2**) (Figure 1) isolated from the phytopathogenic fungus *Pyrenophora avenae*[7] and *Stemphylium radicinum*[8] (structure elucidation in ref.[6]).

  

### Bioactivity

The pure compounds were tested against the Gram-positive bacterium *Bacillus megaterium*, the fungus *Microbotryum violaceum,* and the alga *Chlorella fusca* (Table 1). Pyrenophorol (**1**) was reported to show anthelmintic properties.[2] In our test it was moderately active against the fungus *Microbotryum violaceum*. The carboxylic acid **4** had moderate algicidal properties, but both compounds were inactive against *Bacillus megaterium*. There were not adequate quantities of metabolites to test for herbicidal activity.

Table 1. Activity of compounds **1** and **4** against the Gram-positive bacterium *Bacillus megaterium,* the fungus *Microbotryum violaceum,* and the algae *Chlorella fusca*.[a]

| | *Bacillus megaterium* | *Microbotryum violaceum* | *Chlorella fusca* |
|---|---|---|---|
| **1** | – | 8, gi[b] | – |
| **4** | – | – | 6, gi |

[a] Application of 50 μL of a 10 mg/mL (**1**) or 5 mg/mL (**4**) solution in an agar diffusion test. Radii of zones of inhibition are given in mm. [b] gi indicates that some growth occurred in the zone of inhibition.

## Conclusion

The absolute configuration of tetrahydropyrenophorol (**3**), a new member of the diolide macrolactone family, was established by the new solid-state TDDFT CD methodology. The simultaneous isolation of pyrenophorol (**1**), tetrahydropyrenophorol (**3**) and pyrenophorolic acid (**4**) suggested their biogenetic relationship and identical relative and absolute configuration. It is noteworthy that CD spectra measured for compound **3** in solution and in the solid state differed in sign due to molecular flexibility in solution. The current example demonstrates the advantages of the solid-state TDDFT/CD methodology compared to the conventional solution CD method.

## Experimental Section

For general methods and instrumentation see ref.[35] and for microbiological methods and conditions of culture see ref.[36] Melting points were determined on a Gallenkamp micro-melting point apparatus and are uncorrected. NMR spectra were recorded on a Bruker-500 NMR avance spectrometer. EIMS were obtained on a MAT 8200 mass spectrometer. Compounds were detected on TLC plates (Merck AG, silica gel 60 $F_{254}$) by spraying with cerium-molybdenum spray reagent followed by heating. CD spectra were recorded on a J-810 spectropolarimeter, and the concentrations are given in mol/dm$^3$. For the solid-state CD measurement, the disc was prepared by mixing 181 mg KCl (optical grade, random crystals, 99.98%, Aldrich, heated at 100 °C) and 204 μg of **3** with a Perkin–Elmer vibrating mill for 5 min producing a fine powder to minimize the dispersion and absorption flattening effects. Then the mixture was pressed at 10 tons with a Perkin–Elmer press under vacuum to obtain a transparent disc for CD measurements.

**Isolation:** Fungal strain 7217 was cultivated at room temperature for 25 d on biomalt solid agar medium. The broth was extracted four times with ethyl acetate to obtain the crude extracts (6.5 g) that were subjected to column chromatography on silica gel, using petroleum ether/dichloromethane, then dichloromethane and then gradients of dichloromethane with up to 10% methanol. On the basis of TLC, similar fractions were combined and investigated to isolate the following pure compounds: 20.9 mg of of **1** (hexane/ethyl acetate, 3:7, $R_f$ = 0.71), 18.9 mg of **3** (hexane/ethyl acetate, 3:7, $R_f$ = 0.65), 33.3 mg of **4** (hexane/ethyl acetate, 34:7, $R_f$ = 0.50).

**Data for Pyrenophorol (1):** M.p. 130–132 °C. IR (KBr): $\tilde{\nu}$ = 3325, 2983, 2945, 2868, 1716, 1650, 1449, 1357, 1270, 1172, 1117 cm$^{-1}$. UV ($CHCl_3$): $\lambda_{max}$ (log $\varepsilon$) = 266 nm (198) cm$^{-1}$. $[\alpha]_D^{22}$ = –13.3 ($c$ = 0.11, $CHCl_3$), ref.[2] $[\alpha]_D^{22}$ = –14.9 ($c$ 1, $CHCl_3$). $^1$H NMR (500 MHz, $CDCl_3$): $\delta$ = 1.26 (d, $J$ = 6.5 Hz, 3 H, 8-$CH_3$), 1.63 (m, 1 H, 6-H), 1.71 (m, 1 H, 6-H), 1.85 (m, 2 H, 5-H), 4.25 (m, 1 H, 4-H), 5.10 (m, 1 H, 7-H), 5.95 (d, $J$ = 15.7 Hz, 1 H, 2-H), 6.89 (dd, $J$ = 15.7, 5.7 Hz, 1 H, 3-H) ppm. $^{13}$C NMR (125 MHz, $CDCl_3$): $\delta$ = 18.4 (C-8), 28.9 (C-6), 30.7 (C-5), 69.9 (C-7), 70.4 (C-4), 122.1 (C-2), 149.2 (C-3), 165.2 (C-1) ppm. EIMS (70 eV, 200 °C): $m/z$ (%) = 156 (61) [M]$^+$, 139 (100), 138 (89), 111 (63), 93 (39), 84 (37), 73 (15), 55 (53).

**Data for Tetrahydropyrenophorol (3):** M.p. 124–127 °C. IR (KBr): $\tilde{\nu}$ = 3418, 2988, 2912, 2847, 1732, 1705, 1449, 1373, 1335, 1270, 1166 cm$^{-1}$. $[\alpha]_D$ = –68 ($c$ = 0.14, $CHCl_3$). UV ($CH_3CN$): $\lambda_{max}$ (log $\varepsilon$) = 199 (2.39), 213 sh (2.30). CD ($CH_3CN$, $c = 7.1 \times 10^{-4}$): $\lambda$ ($\Delta\varepsilon$) = 209 nm (0.92). CD (MeOH, $c = 8.2 \times 10^{-4}$): $\lambda$ ($\Delta\varepsilon$) = 208 nm (1.06). CD (KCl): $\lambda$ ($\Delta\varepsilon$) = 213 nm (–2.5). $^1$H NMR (500 MHz, $CDCl_3$): $\delta$ = 1.23 (d, $J$ = 6.2 Hz, 3 H, 8-$CH_3$), 1.37 (m, 1 H, 5-H), 1.52 (m, 1 H, 5-H), 1.72 (m, 2 H, 3-H), 1.79 (m, 1 H, 6-H), 1.86 (m, 1 H, 6-H), 2.45 (m, 2 H, 2-H), 3.56 (m, 1 H, 4-H), 5.03 (m, 1 H, 7-H) ppm. $^{13}$C NMR (125 MHz, $CDCl_3$): $\delta$ = 20.0 (C-8), 30.7 (C-2), 30.8 (C-5), 31.1 (C-6), 33.1 (C-3), 68.0 (C-4), 69.6 (C-7), 173.4 (C-1) ppm. EIMS (70 eV, 200 °C): $m/z$ (%) = 159 (53) [M + H]$^+$, 157 (12), 141 (100), 123 (33), 99 (45), 85 (71), 81 (19).

**Crystal Structure Determination of 3:**[37] $C_{16}H_{28}O_6$, $Mr$ = 316.4, orthorhombic, space group $P2_12_12_1$, $a$ = 10.5718(15), $b$ = 12.1771(17), $c$ = 12.9481(18) Å, $V$ = 1666.9(4) Å$^3$, $Z$ = 4, $D_x$ = 1.261 g/cm$^3$, $F$(000) = 688, $T$ = 120(2) K. Bruker-AXS SMART APEX CCD,[37] graphite monochromator, $\lambda$(Mo-$K_\alpha$) = 0.71073 Å, $\mu$ = 0.09 mm$^{-1}$, colorless crystal, size 0.50 × 0.48 × 0.40 mm$^3$, 16593 intensities collected $2.5 < \theta < 28.2°$, $-14 < h < 13$, $-16 < k < 16$, $-17 < l < 17$. Structure solved by direct methods,[38] full-matrix least-squares refinement[38] with 2331 independent reflections based on $F^2$ and 202 parameters, all but H atoms refined anisotropically, H atoms from difference Fourier maps refined with riding model on idealized positions with $U = 1.5\,U_{iso}$(O and methyl-C) or $1.2\,U_{iso}$(C). **3** crystallizes in the non-centrosymmetric space group $P2_12_12_1$; however, in the absence of significant anomalous scattering effects, the Flack[39] parameter is essentially meaningless. Accordingly, Friedel pairs were merged. Refinement converged at $R_1[I > 2\sigma(I)]$ = 0.041, $wR_2$(all data) = 0.112, $S$ = 1.13, max.($\delta/\sigma$) < 0.001, min./max. height in final $\Delta F$ map –0.19/0.26 e/Å$^3$. Figure 2 shows the molecular structure.

**Data for (4*S*,7*R*)-4,7-Dihydroxyoctanoic Acid (4, Pyrenophorolic Acid):** IR (KBr): $\tilde{\nu}$ = 3505, 3407, 2961, 2917, 2852, 1754, 1454, 1362, 1286, 1183 cm$^{-1}$. $[\alpha]_D$ = –71.7 ($c$ = 0.29, $CHCl_3$). $^1$H NMR (500 MHz, $CDCl_3$): $\delta$ = 1.22 (d, $J$ = 7 Hz, 3 H, 8-$CH_3$), 1.55–1.64 (m, 2 H, 6-H), 1.71 (m, 1 H, 5-H), 1.87 (m, 1 H, 5-H), 1.90 (m, 1 H, 3-H), 2.34 (m, 1 H, 3-H), 2.54 (m, 2 H, 2-H), 3.86 (m, 1 H, 7-H), 4.55 (m, 1 H, 4-H) ppm. $^{13}$C NMR (125 MHz, $CDCl_3$): $\delta$ = 23.7 (C-8), 27.9 (C-3), 28.8 (C-2), 31.6 (C-5), 34.3 (C-6), 67.3 (C-7), 80.7 (C-4), 177.1 (C-1) ppm. EIMS (70 eV, 200 °C): $m/z$ (%) =

  

177 (5) $[M + H]^+$,167 (14), 159 (77), 141 (85), 123 (60), 85 (100), 81 (37), 55 (27), 53 (24).

**Computational Section:** MMFF conformational searches were run with the Monte-Carlo algorithm included in the Spartan'06 program (Wavefunction, Inc., Irvine CA, 2006), using default parameters and convergence criteria. AM1 geometry optimizations were run on all conformers obtained through MMFF conformational search within 10 kcal/mol. DFT and TDDFT calculations were run with the Gaussian′03 program (Gaussian, Inc., Pittsburgh PA, 2003). The input geometry for TDDFT calculations was obtained from the solid-state structure upon re-optimization of the H-atoms' positions with the DFT method at the B3LYP/6-31G(d) level. TDDFT calculations were executed employing 1) the hybrid functionals B3LYP, PBE0 (PBE1PBE) and BH&HLYP, and 2) native Ahlrich's TZVP or Dunning's aug-cc-pVDZ basis sets, or else the "aug-TZVP" basis set obtained from TZVP augmented with a set of Dunning-type diffuse functions.[26] CD spectra were generated using dipole length-computed rotational strengths to which a Gaussian band-shape was applied with 6,000 $cm^{-1}$ half-height width (corresponding to 26.5 nm at 210 nm).

**Supporting Information** (see also the footnote on the first page of this article): Relevant dihedral angles for AM1-optimized structures of tetrahydropyrenophorol (**3**) within 2 kcal/mol, and estimated contribution to CD signal at 210 nm according to modified Snatzke's comet rule, compared with TDDFT-computed rotational strengths (B3LYP/3-21G(d)) for the chromophoric fragments (like **5**) extracted from the first 10 minima (<1 kcal/mol).

## Acknowledgments

K. K., I. K., B. S. and S. D. thank BASF AG and the Bundesministerium für Bildung und Forschung (BMBF), project no. 03F0360A, and S. A. and T. K. thank the Hungarian Scientific Research Fund (OTKA, T-049436, F-043536, NI-61336) for financial support. Prof. A. Zeeck is thanked for kindly providing a sample of pyrenophorol (helmidiol) (**1**).

[1] I. Kock, K. Krohn, H. Egold, S. Draeger, B. Schulz, J. Rheinheimer, *Eur. J. Org. Chem.* **2007**, in print.
[2] R. Kind, A. Zeeck, S. Grabley, R. Thiericke, M. Zerlin, *J. Nat. Prod.* **1996**, *59*, 539–540.
[3] E. L. Ghisalberti, J. R. Hargreaves, B. W. Skelton, A. H. White, *Aust. J. Chem.* **2002**, *55*, 233–236.
[4] Z. Kis, P. Furger, H. P. Sigg, *Experientia* **1969**, *25*, 123–124.
[5] J. F. Grove, *J. Chem. Soc., C* **1971**, 2261–2263.
[6] S. Nozoe, K. Ilirai, K. Tsuda, K. Ishihashi, M. Shirasaka, *Tetrahedron Lett.* **1965**, *6*, 4675–4677.
[7] K. Ishibashi, *J. Agric. Chem. Soc. Jpn.* **1961**, *35*, 257–262.
[8] J. F. Grove, *J. Chem. Soc.* **1964**, 3234.
[9] M. A. Kastanias, M. Chrysayi-Tokousbalides, *J. Agric. Food Chem.* **2005**, *53*, 5943–5947.
[10] C. Christner, G. Kullertz, G. Fischer, M. Zerlin, S. Grabley, R. Thiericke, A. Taddei, A. Zeeck, *J. Antibiot.* **1998**, *51*, 368–371.
[11] F. J. Dommerholt, L. Thijs, B. Zwanenburg, *Tetrahedron Lett.* **1991**, *32*, 1499–1502.
[12] N. Machinaga, C. Kibayashi, *Tetrahedron Lett.* **1993**, *34*, 841–844.
[13] D. Seebach, B. Seuring, H.-O. Kalinowski, W. Lubosch, B. Renger, *Angew. Chem.* **1977**, *89*, 270–271; *Angew. Chem. Int. Ed.* **1977**, *16*, 264–265.
[14] S. Hatakeyama, K. Satoh, K. Sakurai, S. Takano, *Tetrahedron Lett.* **1987**, *28*, 2717.
[15] S. Amigoni, Y. Le Floc'h, *Tetrahedron: Asymmetry* **1997**, *8*, 2827–2831.
[16] B. Elsässer, K. Krohn, U. Flörke, N. Root, H.-J. Aust, S. Draeger, B. Schulz, S. Antus, T. Kurtán, *Eur. J. Org. Chem.* **2005**, 4563–4570.
[17] H. Hussain, K. Krohn, U. Flörke, B. Schulz, S. Draeger, G. Pescitelli, S. Antus, T. Kurtán, *Eur. J. Org. Chem.* **2007**, 292–295.
[18] K. Krohn, I. Kock, B. Elsässer, U. Flörke, B. Schulz, S. Draeger, G. Pescitelli, S. Antus, T. Kurtán, *Eur. J. Org. Chem.* **2007**, in print.
[19] G. Bringmann, S. Busemann, *The Quantummechanical Calculation of CD Spectra: the Absolute Configuration of Chiral Compounds from Natural or Synthetic Origin* in *Natural Product Analysis, Chromatography, Spectroscopy, Biological Testing* (Eds.: P. Schreier, M. Herderich, H.-U. Humpf, W. Schwab), Vieweg & Sohn Verlagsgesellschaft, Braunschweig, Wiesbaden, **1998**, pp. 195–211.
[20] C. Diedrich, S. Grimme, *J. Phys. Chem. A* **2003**, *107*, 2524–2539.
[21] T. D. Crawford, *Theor. Chem. Acc.* **2006**, *115*, 227–245.
[22] A. Dreuw, M. Head-Gordon, *Chem. Rev.* **2005**, *105*, 4009–4037.
[23] M. A. L. Marques, E. K. U. Gross, *A Primer in Density Functional Theory* in *Lecture Notes in Physics, Time-Dependent Density Functional Theory* (Eds.: C. Fiolhais, F. Nogueira, M. A. L. Marques), vol. 620, Springer-Verlag, Berlin, **2003**, pp. 144–184.
[24] R. Kuroda, *Circular Dichroism in the Solid State*, in *Chiral Photochemistry* (Eds.: Y. Inoue, V. Ramamurthy), Dekker, New York **2004**, pp. 385–413.
[25] M. E. Casida, C. Jamorski, K. C. Casida, D. R. Salahub, *J. Chem. Phys.* **1998**, *108*, 4439–4449.
[26] See Gaussian′03 documentation (http://www.gaussian.com/g_ur/g03mantop.htm) for details on basis sets and DFT functionals.
[27] L. Di Bari, S. Guillarme, S. Hermitage, D. A. Jay, G. Pescitelli, A. Whiting, *Chirality* **2005**, *17*, 323–331.
[28] M. Pecul, K. Ruud, T. Helgaker, *Chem. Phys. Lett.* **2004**, *388*, 110–119.
[29] *Fundamentals Aspects and Recent Developments in Optical Rotatory Dispersion and Circular Dichroism* (Eds.: F. Ciardelli, P. Salvadori), Heiden, London, **1973**.
[30] G. Snatzke, *Angew. Chem.* **1979**, *91*, 380–393; *Angew. Chem. Int. Ed. Engl.* **1979**, 363–377.
[31] W. Klyne, P. M. Scopes, *The Carboxyl and Related Chromophore* in *Fundamental Aspects and Recent Developments*, in *Optical Rotatory Dispersion and Circular Dichroism* (Eds.: F. Ciardelli, P. Salvadori), Heiden, London, **1973**, p. 126 ff.
[32] G. Snatzke, H. Ripperger, C. Horstmann, K. Schreiber, *Tetrahedron* **1966**, *22*, 3103–3116.
[33] W. Priyono Suwarso, R. Layla Gani, K. Krohn, M. John, *Eur. J. Org. Chem.* **1999**, 1719–1721.
[34] U. Flörke, W. Priyono Suwarso, R. L. Gani, K. Krohn, S. Wang, *Acta Crystallogr., Sect. E* **2003**, *59*.
[35] J. Dai, K. Krohn, D. Gehle, I. Kock, U. Flörke, H.-J. Aust, S. Draeger, B. Schulz, J. Rheinheimer, *Eur. J. Org. Chem.* **2005**, 4009–4016.
[36] B. Schulz, C. Boyle, S. Draeger, H.-J. Aust, A.-K. Römmert, K. Krohn, *Mycolog. Res.* **2002**, *106*, 996–1004.
[37] CCDC-629777 (for **3**) contains the supplementary crystallographic data for this paper. These data can be obtained free of charge from The Cambridge Crystallographic Data Centre via www.ccdc.cam.ac.uk/data_request/cif.
[38] SMART (ver. 5.62), SAINT (ver. 6.02), SHELXTL (ver. 6.10) and SADABS (ver. 2.03), Bruker AXS Inc., Madison, Wisconsin, USA, **2002**.
[39] H. D. Flack, *Acta Crystallogr., Sect. A* **1983**, *39*, 876–881.

Received: December 27, 2006
Published Online: May 4, 2007

  